ChemComm

COMMUNICATION

View Article Online
View Journal | View Issue

Cite this: *Chem. Commun.*, 2020, **56**, 13343

Received 1st September 2020,
Accepted 29th September 2020

DOI: 10.1039/d0cc05921h

rsc.li/chemcomm

In silico design of novel NRR electrocatalysts: cobalt–molybdenum alloys†

Blanca Castellano-Varona,[a] Moussab Harb,[b] Javier Araña,[a] Luigi Cavallo *[b] and Luis Miguel Azofra *[a]

Metals are amongst the most efficient developed electrocatalysts for nitrogen reduction reaction (NRR) with iron and ruthenium presenting the best catalytic indicators. However, the potential use of metal alloys as NRR electrocatalysts is still underdeveloped. While Co has demonstrated poor electrocatalytic activity for NRR, alloying Co with Mo exhibits an improvement in both N_2 physisorption and the stabilisation of the elusive N_2H as the first reduced intermediate species. This stabilisation occurs on surface Mo or Co atoms with a high connectivity with Mo. Herein, we report a complete DFT study analysing the potential application of CoMo alloys as catalysts for N_2-into-NH_3 conversion given the low theoretical overpotentials that they present.

The Haber–Bosch process[1] has been considered as the most important technological marvel of the last century[2] due to the use of ammonia (NH_3) as the source of most fertilisers. Since large-scale NH_3 synthesis demands very harsh operation conditions of temperature (350–525 °C) and pressure (100–300 atm),[3] it is estimated that the Haber–Bosch process nearly contributes 2% of the global CO_2 greenhouse gas emissions. In order to mitigate this enormous carbon footprint, the production of "green ammonia" has been rapidly intensified.[4,5]

Electrosynthesis of NH_3 from air sourced N_2 has demonstrated promising prospects for the development of small-scale machineries capable of producing green ammonia at mild conditions.[6] A plethora of novel electromaterials capable of catalysing the nitrogen reduction reaction (NRR) has been reported in the recent years,[7] albeit controversies have arisen because of the lack of proper protocols for ammonia quantification in most of these experimental studies.[8] One of the elements of greatest inspiration for the design of novel NRR catalysts has been the iron-molybdenum cofactor (FeMoco) of nitrogenase enzymes.[9] In this direction, the development of homogeneous catalysts mimicking FeMoco has been the subject of investigations with notable impact.[10,11] Additional efforts, however, have been focused on the development of heterogeneous electrocatalysts, a field of great interest and application in which our groups are deeply involved.

Amongst the variety of developed electrocatalysts for NRR, the use of metals has occupied a prominent position. In this context, MacFarlane and co-workers reported the synthesis of a nanostructured iron material combined with an aprotic fluorinated solvent–ionic liquid mixture exhibiting NH_3 yield rate of 16 mg h^{-1} m^{-2}.[12] Contemporaneously to the Nørskov's findings,[13] this work was the pioneer in the use of water as the only proton source. Recent contributions from our groups involved the synthesis of α-Fe nanorods supported on carbon fibre revealing high NRR faradaic efficiency of 32%.[14] The testing of ruthenium nanoparticles showed the capability of converting N_2 into NH_3 at very low overpotential of −100 mV *vs.* RHE[15] compared to others.[16]

Despite metallic materials have demonstrated outstanding abilities for mild conditions nitrogen fixation, the use of metal alloys as potential NRR electrocatalysts is still underdeveloped and only few testimonial works have been recently published.[17–20] Getting encouraged also by our interests in the *in silico* design of novel NRR materials, we report that cobalt–molybdenum alloys exhibit promising prospects for the stabilisation of nitrogen intermediates during NRR, an unprecedented behaviour that we analyse from a DFT-based mechanistic perspective.

NRR is a process occurring at mild conditions of temperature and pressure as consequence of a mechanism characterised by the successive transfer of six protons and electrons to N_2 for producing NH_3 *via* an associative pathway. Fig. 1 displays the minimum energy path for the metal-catalysed NRR, in which the metal species is situated on the (001) surface of epsilon cobalt (ε-Co), *i.e.*, a hexagonal close-packed (hcp) structure. The Co atoms in the (001) surface of ε-Co are geometrically disposed forming angles of 60° and 120° with their neighbouring atoms

[a] *Instituto de Estudios Ambientales y Recursos Naturales (i-UNAT), Universidad de Las Palmas de Gran Canaria (ULPGC), Campus de Tafira, 35017, Las Palmas de Gran Canaria, Spain. E-mail: luismiguel.azofra@ulpgc.es*

[b] *KAUST Catalysis Center (KCC), King Abdullah University of Science and Technology (KAUST), Thuwal 23955-6900, Saudi Arabia. E-mail: luigi.cavallo@kaust.edu.sa*

† Electronic supplementary information (ESI) available: Full computational details and optimised Cartesian coordinates. See DOI: 10.1039/d0cc05921h

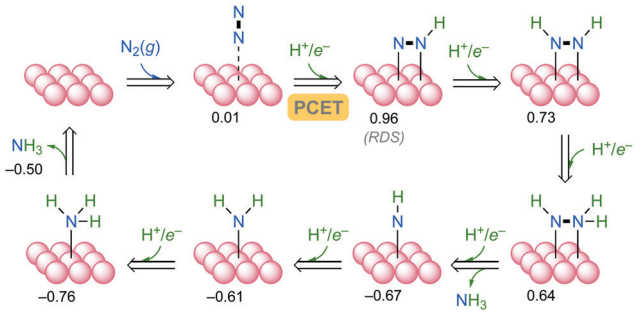

Fig. 1 Reaction mechanism for NRR catalysed by ε-Co(001). Free energies are shown in eV at RTP conditions when there is not applied bias (U = 0 V) and pH = 0 (CHE).

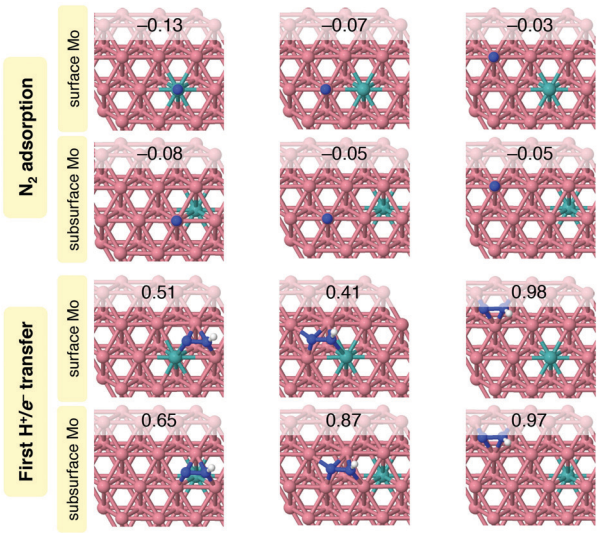

Fig. 2 Top view of key adsorption possibilities of both N_2 and N_2H species on ε-Co(001) surface when doped with one Mo atom at the surface and subsurface (second layer). Free energies are shown in eV. Pink, green, blue, and white spheres refer to Co, Mo, N, and H atoms, respectively.

and exhibiting an electropositive character that might propitiate the interaction of N_2 and their intermediate reduced species over them. For this specific case, our results indicate that N_2 physisorption on ε-Co(001) is slightly endergonic with a binding free energy of 0.01 eV. In the framework of the proton-coupled electron transfer (PCET) approach, *i.e.*, both proton and electron reach the catalytic surface in a concerted way,[21,22] the first hydrogenation step comprising the $*N_2 + H^+/e^- \rightarrow *N_2H$ elementary step is 0.96 eV *vs.* the computational hydrogen electrode (CHE). (See full computational details at ESI†). N_2H species is adsorbed onto the (001) surface of cobalt acquiring a side-on disposition with proximal Co–N and Co–N(H) distances of 1.85 and 1.94 Å, respectively. (See Fig. S2 at ESI†). In terms of relative energies, the free energy difference between the $*N_2H$ and $*N_2$ states (where '*' denotes the catalytic surface) is 0.95 eV. In other words and assuming no extra kinetics cost, the first reduction step of N_2 catalysed by ε-Co(001) is hypothesised to occur at a cathodic overpotential of −950 mV *vs.* SHE (pH = 0). The reaction continues with the formation of the *NHNH, $*NHNH_2$, *NH, $*NH_2$, and $*NH_3$ adsorbates with the respective release of two NH_3(g) molecules. In all these cases, the energy required at each step is lower than the energy demanded to produce N_2H, revealing that the first hydrogenation (with relative free energy of 0.95 eV) is the rate-determining step (RDS) of the whole process attending to DFT data.

We have also explored the N_2 adsorption and the first hydrogenation step catalysed by γ-Co(111), *i.e.*, the analogous surface to ε-Co(001) for the face-centred cubic (fcc) structure. Free energies of 0.00 and 0.95 eV were obtained in each case (Fig. S2 at ESI†), which reveals a minor or unnoticeable effect of the atomic packing. Thus, metallic cobalt in any of its stable allotropic ε and γ forms exhibits a moderate catalytic behaviour in the stabilisation of the N_2H species. However, from an energetic point-of-view, this still remains far from benchmarking materials such as iron[14] or ruthenium.[15,23]

Within *in silico* design strategies, we were wondering about the effect in the NRR catalysis by mixing cobalt with other transition metals in low proportion. Amongst all the possibilities, molybdenum emerges as one of the most promising candidates given its activity in N_2 conversion.[24–27]

Surprisingly, molybdenum offered promising scenarios when testing the effect of both, the doping with one molybdenum atom at the surface and the subsurface (second layer) of ε-Co(001). Fig. 2 details N_2 adsorption and first H^+/e^- transfer to form the N_2H species.

Doping cobalt with one Mo atom has favouring effects in the adsorption of N_2. Interestingly, both surface and subsurface Mo atoms lead to spontaneous binding free energies for the interaction of N_2, which acquires an end-on disposition in all cases. This effect is more pronounced when N_2 directly interacts with Mo (−0.13 eV), revealing that the farther from the Mo atom the less spontaneous binding energy. Similarly, it is also observed that N_2H species is more stabilised when this binds with the Mo atom. Because N_2H species has two binding points with the surface, it has been observed that the existence of the Mo–N(H) motif (0.41 eV *vs.* CHE) leads to a more favourable minimum than the Co–N(H) (0.51 eV *vs.* CHE).

With molybdenum playing a principal role in the stabilisation of the N_2H species, and therefore increasing the catalytic efficiency of the material, we were wondering if a larger number of Mo atoms within the Co crystal lattice would have a greater effect. First, modelling alloys involve the proposition of a huge number of 'initial guesses', *i.e.*, set of structures each one with an inequivalent arrangement of the atoms. This difficult task also involves an enormous amount of computational resources. In order to simplify this, we have prepared models in which the fourth and fifth inner layers are only constituted by cobalt while the rest are mixed with a 90 : 10 proportion of Co : Mo atoms, which takes into account such inners layers resulting from slabs with formula $Co_{113}Mo_{12}$. Thus, we have proposed a thousand of initial structures where the molybdenum atoms have been randomly placed.

Fig. 3 displays the atomic dispositions of the upper three layers in the three most (**a–c**) and less (**d–f**) stable structures obtained after optimisation. Comparing, for instance, structures **a** and **d**, two patterns of stability are clearly revealed: lower

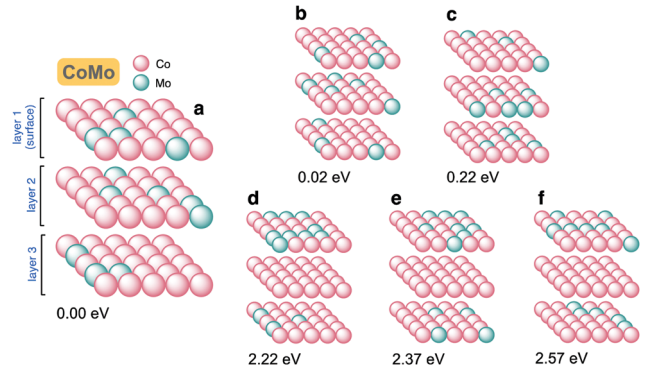

Fig. 3 Atomic dispositions of the three layers at top in a set of slabs of 90 : 10 CoMo alloys.

energy structures tend to an equal distribution of the Mo atoms in the three layers with Mo–Mo linkages disfavouring the stability. Thus, minimum **a** (0.00 eV) have 4, 5, and 3 Mo atoms in the upper layers and 4 Mo–Mo bonds per unit cell while minimum **d** (2.22 eV) have 9 and 3 Mo atoms only in the first and third layers and 9 Mo–Mo bonds. It might appear that structure **b** (0.02 eV) should have greater stability than **a** given the apparent absence of Mo–Mo linkages, however they are mostly interlayer.

All these aspects concerning the analysis of the atomic packaging in alloys are of interest. However, other questions of relevance are also raised regarding the catalytic behaviour given that alloy surfaces are not uniform. In this sense, the already described minimum for the adsorption of the N_2H species in ε-Co is a representative structure since this will be the lowest energy conformation at any point of the (001) surface. In the alloy surface, a variety of motifs can be found, so it is expected that each local area in the surface exhibits a differentiated catalytic character.

Fig. 4 specifies an atomic ordering of the 25 atoms constituting the (001) surface of the aforementioned structure **a**. Thus, indexes **D**, **F**, **G**, and **R** represent Mo atoms while the rest are Co. The first value of each pair represents the free energy for the (end-on) N_2 adsorption and these binding energies have been accounted in −0.16, −0.16, −0.17, −0.12 eV, respectively. As can be seen, we observe a similar behaviour as in the model system constituted by one surface Mo, in which ΔG_b = −0.13 eV (Fig. 2). This means that surface Mo atoms on this 90 : 10 CoMo alloy are electropositive centres favouring the spontaneous physisorption of N_2. Surprisingly, the most exergonic value is observed in centre **J** corresponding to a cobalt atom (−0.26 eV), which is connected with two surface Mo atoms plus another one placed in the second layer. Again, and as we observed in the model cases shown in Fig. 2, this stabilisation of the N–M (M = metal) bond is not solely due to the direct interaction between N_2 and Mo, but to Co atoms being also connected with Mo centres. In this context, the closer the cobalt atoms are connected to molybdenum the greater the spontaneity of that interaction. Undoubtedly, these data provide relevant information for the purposes of the *in silico* design of novel

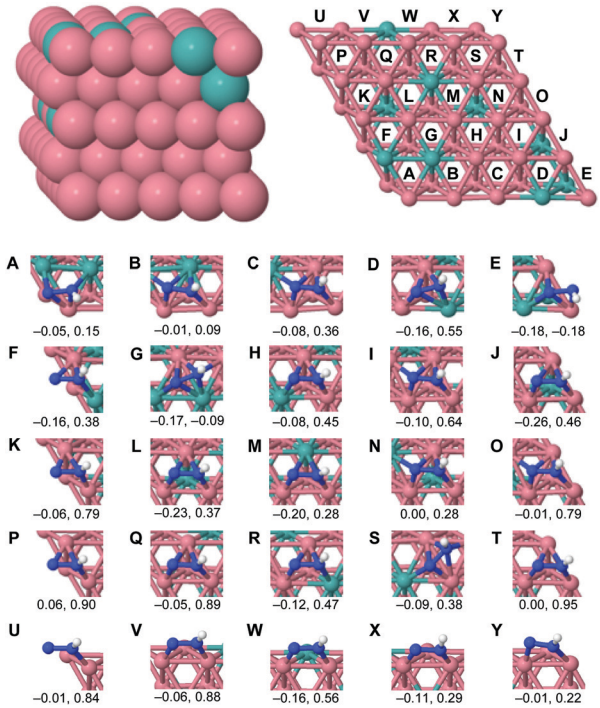

Fig. 4 Side and top views for minimum a of 90 : 10 CoMo alloy and adsorbed N_2H species at different points of the (001) surface. Two energies, in eV, are shown: adsorption of N_2 and N_2H species, respectively.

NRR catalysts, where a material without N_2 adsorption capacity becomes active upon the inclusion of Mo into Co to form a CoMo alloy. In this context, the interaction of N_2 with the catalytic surface is a fundamental prerequisite to start the catalytic process.

Since N_2H species exhibits a side-on conformation, it binds with the two N atoms on four metal centres of the surface. Thus, in the first minimum described at Fig. 4, metals at **EAFG** positions are involved in the stabilisation of the N_2H species, and metals at **ABFG** are doing for the second one, *etc.* However, for the sake of greater simplicity we will refer to minima **A**, **B**, **C**, *etc.* As was observed for the adsorption of N_2, it is expected that the N_2H species is more stabilised when interacting with Mo atoms or with Co atoms with a high connectivity with Mo. These are the cases of minima **G** and **E** being the ones that show the lowest values of reaction free energies, specifically −0.09 and −0.18 eV *vs.* CHE. Taking into account the most stable $*N_2$ structure involved with any atom in their surroundings, maximum thermodynamics impediments ($\Delta G^*_{N_2H} - \Delta G^*_{N_2}$) of 0.08 and 0.00(3) eV can be estimated in each case. This information discloses that particular areas of the CoMo alloy surface behave as promising catalytic sides for NRR. They are capable not only of decreasing the reaction energy required to produce the first electrochemical hydrogenation, but also the N_2H interaction which is in the spontaneous regime of free energies. On the contrary, the highest reaction free energies are shown in those cases in which the N_2H is interacting just with surface cobalt atoms as it is the situation in **P** (0.90 eV *vs.* CHE) and **T** (0.95 eV *vs.* CHE) minima. Notwithstanding, a general

view of the energy results shown at Fig. 4 indicates that most N_2H interactions are, to some degree, favoured by the "alloy effect".

Concerning the role of this material in NH_3 desorption, NH_3 binds on surface Co atoms with free binding energies between 0.23 and 0.40 eV, depending on the proximity of these centres to Mo atoms. Slightly more endergonic is the NH_3 desorption when interacting on surface Mo atoms, with ΔG_b values between 0.54 and 0.58 eV. (See Fig. S3 at ESI†). It has been identified that **E** and **G** active sites in the CoMo alloy (Fig. 4) exhibit the highest stabilisation of the elusive N_2H species. An analysis of the complete reaction profile for NRR reveals maximum thermodynamics impediments of just 0.35 and 0.51 eV, respectively, *i.e.*, the thermodynamics cost for the reduction of N_2 into NH_3 is lower than the energy demanded for NH_3 desorption, revealing a high electrocatalytic potential of these materials. Surface poisoning with NH_3 is a common problem in NRR, thus ammonia "desorbents" might be required with the aim of regenerating the catalytic surface. In addition, against the competitive effect of the proton reduction *via* HER, our DFT results suggest that the testing of CoMo materials for NRR would have a greater applicability in solvents that have proven to be more efficient in boosting NRR such as room temperature ionic liquids (RTILs).[12,14]

In summary, we report a DFT study analysing the catalytic role that cobalt molybdenum alloys play in the electrochemical conversion of N_2 into NH_3. Based on results, (001) surface of hcp cobalt (ε-Co) is not an active material for N_2 adsorption, however, N_2 spontaneously fixes onto the surface Mo centres of the optimised models of hcp 90 : 10 CoMo alloys. This is also the case of the N_2H species, which is greatly stabilised in the Mo environment of the CoMo network. In general rules, there are two patterns of stabilisation for the N_2 and N_2H species: when the nitrogen moiety interacts with Mo atoms or with Co atoms with a high connectivity with Mo. Finally, we hope that our results might stimulate further interests in the analysis of alloys as potential metallic catalysts for NRR, a field with great projection although still underdeveloped.

Authors thank the KAUST Supercomputing Laboratory using the supercomputer Shaheen II for providing the computational resources.

Conflicts of interest

There are no conflicts to declare.

Notes and references

1 F. Haber and R. Le Rossignol, Zeitschrift für Elektrochemie und Angew., *Phys. Chem.*, 1913, **19**, 53–72.
2 V. Smil, *Nature*, 1999, **400**, 415.
3 M. Appl, Ullmann's Encycl. Ind. Chem., 2011.
4 B. H. R. Suryanto, H.-L. Du, D. Wang, J. Chen, A. N. Simonov and D. R. MacFarlane, *Nat. Catal.*, 2019, **2**, 290–296.
5 D. R. MacFarlane, J. Choi, B. H. R. Suryanto, R. Jalili, M. Chatti, L. M. Azofra and A. N. Simonov, *Adv. Mater.*, 2020, **32**, 1904804.
6 S. D. Minteer, P. Christopher and S. Linic, *ACS Energy Lett.*, 2019, **4**, 163–166.
7 X. Zhu, S. Mou, Q. Peng, Q. Liu, Y. Luo, G. Chen, S. Gao and X. Sun, *J. Mater. Chem. A*, 2020, **8**, 1545–1556.
8 S. Z. Andersen, V. Čolić, S. Yang, J. A. Schwalbe, A. C. Nielander, J. M. McEnaney, K. Enemark-Rasmussen, J. G. Baker, A. R. Singh, B. A. Rohr, M. J. Statt, S. J. Blair, S. Mezzavilla, J. Kibsgaard, P. C. K. Vesborg, M. Cargnello, S. F. Bent, T. F. Jaramillo, I. E. L. Stephens, J. K. Nørskov and I. Chorkendorff, *Nature*, 2019, **570**, 504–508.
9 S. L. Foster, S. I. P. Bakovic, R. D. Duda, S. Maheshwari, R. D. Milton, S. D. Minteer, M. J. Janik, J. N. Renner and L. F. Greenlee, *Nat. Catal.*, 2018, **1**, 490–500.
10 K. C. MacLeod and P. L. Holland, *Nat. Chem.*, 2013, **5**, 559.
11 I. Čorić and P. L. Holland, *J. Am. Chem. Soc.*, 2016, **138**, 7200–7211.
12 F. Zhou, L. M. Azofra, M. Ali, M. Kar, A. N. Simonov, C. McDonnell-Worth, C. Sun, X. Zhang and D. R. MacFarlane, *Energy Environ. Sci.*, 2017, **10**, 2516–2520.
13 J. M. McEnaney, A. R. Singh, J. A. Schwalbe, J. Kibsgaard, J. C. Lin, M. Cargnello, T. F. Jaramillo and J. K. Nørskov, *Energy Environ. Sci.*, 2017, **10**, 1621–1630.
14 B. H. R. Suryanto, C. S. M. Kang, D. Wang, C. Xiao, F. Zhou, L. M. Azofra, L. Cavallo, X. Zhang and D. R. MacFarlane, *ACS Energy Lett.*, 2018, **3**, 1219–1224.
15 D. Wang, L. M. Azofra, M. Harb, L. Cavallo, X. Zhang, B. H. R. Suryanto and D. R. MacFarlane, *ChemSusChem*, 2018, **11**, 3416–3422.
16 X. Guo, H. Du, F. Qu and J. Li, *J. Mater. Chem. A*, 2019, **7**, 3531–3543.
17 H. Wang, Y. Li, C. Li, K. Deng, Z. Wang, Y. Xu, X. Li, H. Xue and L. Wang, *J. Mater. Chem. A*, 2019, **7**, 801–805.
18 R. D. Kumar, Z. Wang, C. Li, A. V. Narendra Kumar, H. Xue, Y. Xu, X. Li, L. Wang and H. Wang, *J. Mater. Chem. A*, 2019, **7**, 3190–3196.
19 H. Yu, Z. Wang, D. Yang, X. Qian, Y. Xu, X. Li, H. Wang and L. Wang, *J. Mater. Chem. A*, 2019, **7**, 12526–12531.
20 Q. Wang, G. Zheng, S. Hao, X. Liu, J. Zheng, Y. Wang, Z. Su, N. Xu, Y. He, L. Lei and X. Zhang, *ACS Sustainable Chem. Eng.*, 2020, **8**, 44–49.
21 S. Hammes-Schiffer, *Chem. Rev.*, 2010, **110**, 6937–6938.
22 A. A. Peterson, F. Abild-Pedersen, F. Studt, J. Rossmeisl and J. K. Nørskov, *Energy Environ. Sci.*, 2010, **3**, 1311–1315.
23 B. H. R. Suryanto, D. Wang, L. M. Azofra, M. Harb, L. Cavallo, R. Jalili, D. R. G. Mitchell, M. Chatti and D. R. MacFarlane, *ACS Energy Lett.*, 2019, **4**, 430–435.
24 W. W. Weare, X. Dai, M. J. Byrnes, J. M. Chin, R. R. Schrock and P. Müller, *Proc. Natl. Acad. Sci. U. S. A.*, 2006, **103**, 17099–17106.
25 K. Arashiba, Y. Miyake and Y. Nishibayashi, *Nat. Chem.*, 2010, **3**, 120.
26 L. M. Azofra, N. Morlanés, A. Poater, M. K. Samantaray, B. Vidjayacoumar, K. Albahily, L. Cavallo and J.-M. Basset, *Angew. Chem., Int. Ed.*, 2018, **57**, 15812–15816.
27 L. M. Azofra, N. Morlanés, A. Poater, M. K. Samantaray, B. Vidjayacoumar, K. Albahily, L. Cavallo and J.-M. Basset, *Angew. Chem., Int. Ed.*, 2019, **58**, 6476.

